Journal of Hazardous Materials 160 (2008) 337–343

Contents lists available at ScienceDirect

Journal of Hazardous Materials

journal homepage: www.elsevier.com/locate/jhazmat

The removal of an anionic red dye from aqueous solutions using chitosan beads—The role of experimental factors on adsorption using a full factorial design

Antonio R. Cestari*, Eunice F.S. Vieira, Jackeline A. Mota

Laboratory of Materials and Calorimetry, Departamento de Química/CCET, Universidade Federal de Sergipe, CEP 49100-000, São Cristóvão, Sergipe, Brazil

ARTICLE INFO

Article history:
Received 6 November 2007
Received in revised form 24 January 2008
Accepted 1 March 2008
Available online 8 March 2008

Keywords:
Chitosan
Dyes
Adsorption thermodynamics
Factorial designs

ABSTRACT

A factorial design was employed to evaluate the quantitative removal of an anionic red dye from aqueous solutions on epichlorohydrin-cross-linked chitosan. The experimental factors and their respective levels studied were the initial dye concentration in solution (25 or 600 mg L^{-1}), the absence or the presence of the anionic surfactant sodium dodecylbenzenesulfonate (DBS) and the adsorption temperature (25 or 55 °C). The adsorption parameters were analyzed statistically using modeling polynomial equations. The results indicated that increasing the dye concentration from 25 to 600 mg L^{-1} increases the dye adsorption whereas the presence of DBS increases it. The principal effect of temperature did not show a high statistical significance. The factorial results also demonstrate the existence of statistically significant binary interactions of the experimental factors. The adsorption thermodynamic parameters, namely $\Delta_{ads}H$, $\Delta_{ads}G$ and $\Delta_{ads}S$, were determined for all the factorial design results. Exothermic and endothermic values were found in relation to the $\Delta_{ads}H$. The positive $\Delta_{ads}S$ values indicate that entropy is a driving force for adsorption. The $\Delta_{ads}G$ values are significantly affected by an important synergistic effect of the factors and not by the temperature changes alone.

1. Introduction

Chitin is a biodegradable and nontoxic polysaccharide widely spread among marine and terrestrial invertebrates and fungi [1,2]. It is usually obtained from waste materials of the sea food-processing industry, mainly shells of crab, shrimp, prawn and krill. Native chitin occurs in these natural composite materials usually combined with inorganics, proteins, lipids and pigments. Its isolation calls for chemical treatments to eliminate these contaminants [3,4]. By treating crude chitin with aqueous 40–50% sodium hydroxide in the 110–115 °C range chitosan is obtained [5]. Fig. 1 presents a schematic representation of the partially deacetylated chitosan structure. Both biopolymers are chemically similar to cellulose, differing only from the R group attached to carbon 2 of the general carbohydrate structure. Chitin and chitosan are closely related since both are linear polysaccharides containing 2-acetamido-2-deoxy-D-glucopyranose and 2-amino-2-deoxy-D-glucopyranose units joined by $\beta(1 \rightarrow 4)$ glycosidic bonds. Due to the features mentioned, the chemical and physical properties of these polymers are different in nature [6]. The fully deacetylated product is rarely obtained due to the risks of side reactions and chain depolymerization [6,7].

Numerous studies have demonstrated the effectiveness of chitosan and derived products in the uptake of metal cations such as lead, cadmium, copper, and nickel and the uptake of oxyanions as well complexed metal ions. In other areas, chitosan has been employed as an excellent adsorbent for sorption of phenols and polychlorined biphenyls [8], anionic dyes [9], enzymes [10], and in pollution control, as a chelating polymer for binding harmful metal ions [11]. Adsorptions of metals from solutions take place using typically both immobilized nitrogenated and oxygenated Lewis bases of the chitosan structure [1,3]. On the other hand, adsorptions of anionic dyes occur mainly due to the electrostatic interactions between the protonated amine groups on the chitosan ($-NH_3^+$) and the SO_3^- groups of the anionic dyes structures.

The extent of metal and/or dye adsorption depends on the source of chitosan, the degree of deacetylation, the nature of the adsorbate molecules, and solution conditions such as the solvent and the adsorption pH value, which makes experimental procedures the only manner to evaluate the interactive chitosan-adsorbate molecule. Since these studies involve a prohibitively large number of experiments, chemometric procedures based on multivariate statistical techniques are employed here. Statistical methods of experimental design and system optimization such as factorial

* Corresponding author. Tel.: +55 79 21056656; fax: +55 79 21056684.
E-mail address: cestari@ufs.br (A.R. Cestari).

0304-3894/$ – see front matter © 2008 Elsevier B.V. All rights reserved.
doi:10.1016/j.jhazmat.2008.03.004

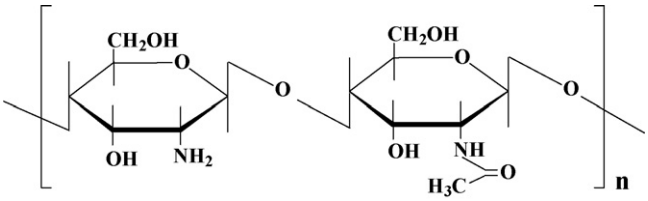

Fig. 1. Structure of partially deacetylated chitosan.

design and response surface analysis have been applied to different adsorption systems because of their capacities to extract relevant information from systems while requiring a minimum number of experiments. Examples of recent applications of the factorial design methodology in adsorption from solution are found, for instance, in the interaction of non-ionic dispersant on lignite particles [12], removal of Ga(III) from aqueous solution using bentonite [13], adsorption of cationic dye on activated carbon beads [14], and optimization of solid-phase extraction and separation of metabolites using HPLC [15]. Since substantial interactions among the experimental adsorption variables are frequently evidenced, which can predominate over main factor effects, univariate optimization strategies have been shown to be relatively inadequate in these kinds of adsorption studies. Besides economizing experimental effort, multivariate methods are capable of measuring interaction effects on metal adsorption as well as the individual effect of each experimental factor on response properties of interest in the most precise way possible. However, to our knowledge, despite the large number of works concerning adsorption of metals and dyes on chitosan, the role of experimental parameter changes on the thermodynamic of adsorption, such as temperature, solute concentration and the presence of micelar interferents, as well as their interactions, are few and scattered.

In this work, chitosan was cross-linked to improve the chemical and mechanical features of raw chitosan. A 2^3 complete factorial design was used to evaluate the importance of three experimental factors concerning the adsorption quantities and the thermodynamical adsorption of an anionic red dye on cross-linked chitosan beads. To determine the statistical significance of the effects, duplicate determinations were made for each of these experiments to evaluate experimental error.

2. Materials and methods

2.1. Materials and characterization of the raw chitosan sample

Water was used after double-distillation. The sulfonated dye Reactive Red RB (abbreviated hereafter as red dye for simplicity), purity of 50%, from The Dystar Company, whose chemical structure is shown in Fig. 2, was used as received. Epichlorohydrin (99%) was from Synth/Brazil and the surfactant sodium dodecylbenzenesulfonate (abbreviated hereafter as DBS for simplicity), 90% of purity, was from Sigma/Aldrich.

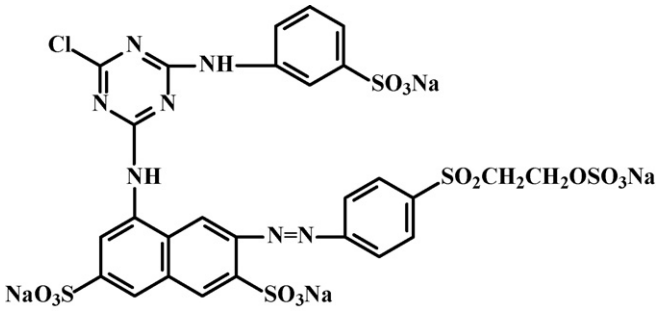

Fig. 2. Chemical structure of the red dye.

Table 1
Factors and levels used in the 2^3 factorial design study

Factors	Levels	
	(−)	(+)
(*C*) = Concentration of the red dye (mg L^{-1})	25	600
(*S*) = Presence of surfactant DBS	No	Yes[a]
(*T*) = Temperature (°C)	25	55

[a] The proportion of DBS/dye was 1:1 in relation to the dye concentration in solution.

The chitosan powder used was from fresh Norwegian shrimp shells from Primex Ingredients A.S. (Norway/Iceland). The following characterizations were performed (details not shown), in order to check some important aspects, concerning the purity and structural aspects of the chitosan sample. Briefly, the degree of deacetylation was determined by infrared spectroscopy [16]. Solid-state ^{13}C NMR spectroscopy was used to verify the purity of the chitosan sample by the positions and their respective intensities of the ^{13}C absorption peaks, from 20 to 200 ppm [11,16]. The total quantity of nitrogen was determined by the Kjeldhal method.

The chitosan beads were synthesized and cross-linked using a 10% (v/v) epichlorohydrin solution as described earlier [4]. Fig. 3 shows a schematic view of the epichlorohydrin-modified chitosan cross-linking reaction. The cross-linked chitosan beads were sieved and used in the 60–100 mesh range and conditioned in a dark air-free flask, in order to prevent possible interactions between the amine groups and atmospheric CO_2 [17].

The determinations of the average density of the beads were made by weighing, separately, 15 beads in an analytical balance. The density of the beads (d) was estimated calculated by the expression $d = m/v$, where m is the mass of the bead and v is its volume, which was calculated as the volume of a perfect sphere. The final results were average values of the 15 densities calculated. FTIR spectra of the chitosan beads, before and after the cross-linking reaction, were taken as KBr pellets using a Bohmen spectrophotometer.

2.2. Adsorption experiments

A full 2^3 factorial design was performed to evaluate the importance of the initial red dye concentration, the presence of the surfactant DBS and temperature on the quantity of dye adsorbed. Table 1 summarizes these factors and their respective levels. The adsorptions of the red dye were performed using a batch procedure [18], where 50 mL of the red dye solutions were agitated for 180 min, sufficient time to reach equilibrium, according to the kinetic isotherms (data not shown), which were performed using the same experimental conditions of each factorial design experiment. In order to increase the red dye removal and to preserve the polymeric chemical structure of the chitosan, the pH values of the solutions were adjusted to 4.0 using a 0.1 mol L^{-1} HCl solution. After a pre-determined contact time, supernatant aliquots were separated by decantation and the red dye concentrations were determined spectrophotometrically at 530 and at 519 nm, in the absence and in the presence of DBS, respectively.

The adsorptions of red dye were calculated using the expression [9,18]:

$$N_f = \frac{(C_i - C_t)V}{m} \quad (1)$$

where N_f is the fixed quantity of dye per gram of chitosan beads at a given time t in mol/g, C_i is the initial concentration of dye in mg/L, C_t

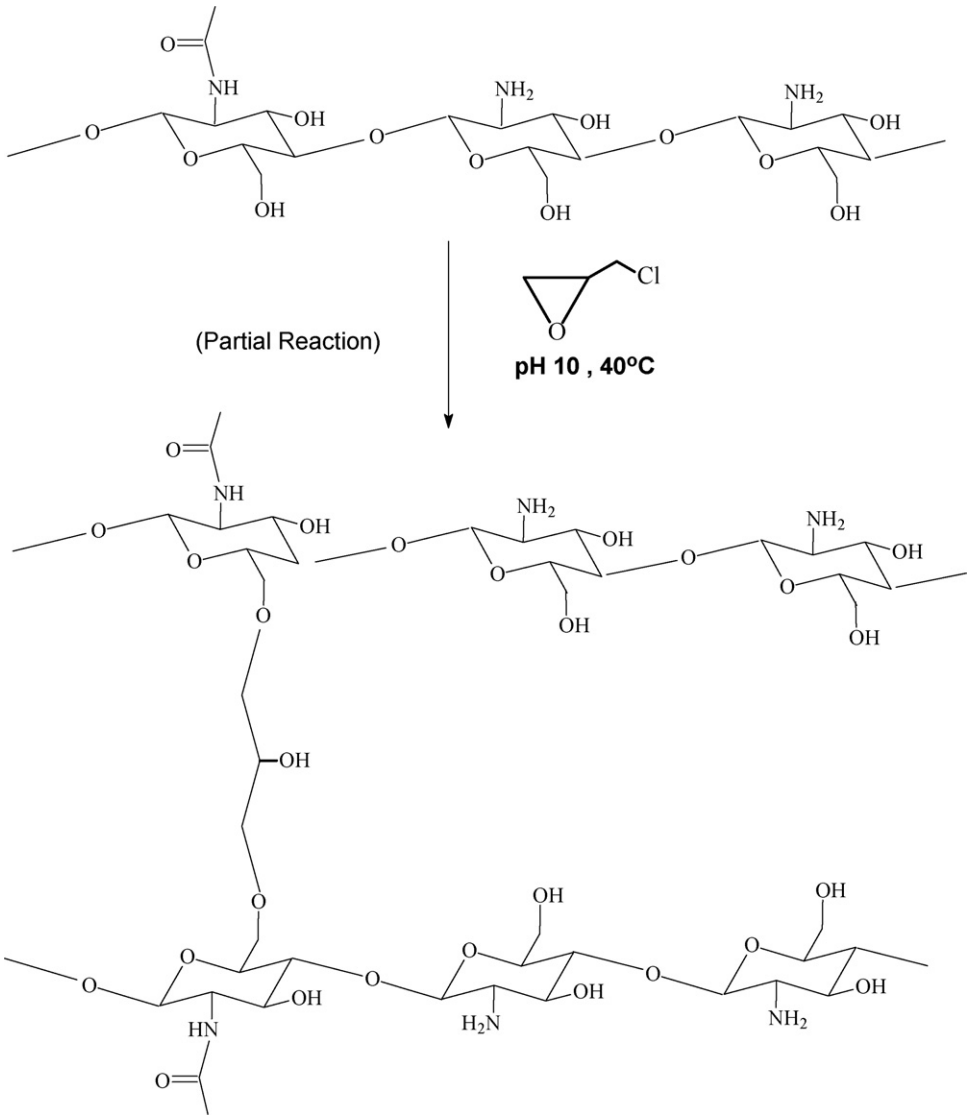

Fig. 3. Partial cross-linking reaction of chitosan using epichlorohydrin. Experimental details: 10% (m/v) of epichlorohydrin aqueous solution; pH 10; stirring time = 3 h; temperature = 40 °C.

is the concentration of dye present at a given time t in mg/L, V is the volume of the solution in L, and m is the mass of beads in grams. Table 2 presents the quantities of dye absorbed for each factorial experiment.

The statistical calculations (t-tests, F-tests, analysis of variance (ANOVA) and multiple regressions) were performed using the software packages ORIGIN®, release 7.0 and the Statistica® release 7.0 [19].

3. Results and discussion

3.1. Initial considerations

The amount of nitrogen of the chitosan, before and after the cross-linking reaction, showed the presence of $6.77 \pm 0.30\%$ (4.84 ± 0.25 mmol g) and $6.47 \pm 0.34\%$ (4.39 ± 0.25 mmol g) of nitrogen. The average densities of the beads were $d = 7.08 \pm 0.34 \times 10^{-4}$

Table 2
Results of the adsorption quantities (N_f) and $\Delta_{ads}G$ of the 2^3 factorial design for the interactions of the red dye with the chitosan beads

Experiment	C	S	T	N_f (mg g^{-1})	N_f(p)[a] (mg g^{-1})	$-\Delta_{ads}G$ (kJ mol^{-1})	$-\Delta_{ads}G$(p)[a] (kJ mol^{-1})
1	−1	−1	−1	3.21	3.06	40.32	42.00
2	1	−1	−1	90.62	88.68	54.35	54.64
3	−1	1	−1	1.47	1.54	39.63	40.96
4	1	1	−1	32.41	35.44	41.80	44.34
5	−1	−1	1	2.05	2.14	43.50	42.00
6	1	−1	1	70.21	73.68	54.06	54.64
7	−1	1	1	0.71	0.62	42.22	40.96
8	1	1	1	23.33	20.44	46.30	44.34

[a] N_f(p) and $-\Delta_{ads}G$(p) represent the adsorption results predicted from Eqs. (4) and (15), respectively.

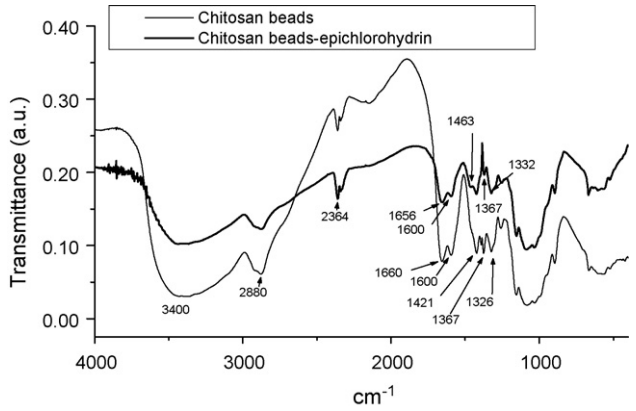

Fig. 4. FTIR spectra of chitosan beads before and after crosslinked with epichlorohydrin.

and $4.10 \pm 0.22 \times 10^{-4}$ g/mm^3 for the beads before and after the cross-linking reaction, respectively. These results reflect a small increase in the ordering of the chitosan chains after the cross-linking reaction [20].

Comparative IR spectra of pristine and epichlorohydrin-crosslinked chitosan beads are shown in Fig. 4. The changes in intensity of the broad band of the hydroxyl groups at about 3400 cm^{-1} of the cross-linked beads show that the hydroxyl groups (—OH) have been consumed for the cross-linking reactions [21] For epichlorohydrin-crosslinked chitosan beads spectrum, the transmittance was reducted at the range of 1000–1300 cm^{-1}, related to C—O stretching vibrations of the chitosan chemical structure. In addition to this, the presence of a small peak at 1463 cm^{-1} in this spectrum, related to secondary amine groups, suggest the possibility that the nitrogen atoms in the carbon C-2 groups of chitosan were also involved in the cross-linking reaction in a small extension.

3.2. Factorial designs calculations

3.2.1. Analysis of the adsorption factors and modeling of the quantitative adsorption of red dye on the chitosan beads

The initial dye concentration, pH, temperature, the presence of surfactants and other experimental factors, have been shown to be significant in the adsorption of dyes taking into account their environmental impact, at dye trace levels [22]. Note that the factors used in this work have never been investigated simultaneously using factorial designs, and they were chosen for their importance, as determined previously using one-variable-at-a-time experimental procedures [1]. The experiments were executed in random order to correctly evaluate experimental errors [23].

Principal and interaction effect values are easily calculated from factorial design results. Both types of effects are calculated using the Eq. (2) [23].

$$\text{Effect} = \bar{R}_{+,i} - \bar{R}_{-,i} \quad (2)$$

where $\bar{R}_{+,i}$ and $\bar{R}_{-,i}$ are average values of N_f for the high (+) and low (−) levels of each factor. For principal or main effects, the above averages simply refer to the results at the high (+) and low (−) levels of the factor whose effect is being calculated independent of the levels of the other factors. For binary interactions $\bar{R}_+$ is the average of results for both factors at their high and low levels whereas $\bar{R}_-$ is the average of the results for which one of the factors involved is at the high level and the other is at the low level. In general, high-order interactions are calculated using the above equation by applying signs obtained by multiplying those for the factors involved (+) for high and (−) for low levels. If duplicate runs are performed for each individual measurement, as done in this work, standard errors (E) in the effect values can be calculated by [23,24]:

$$E = \left\{ \sum (d_i)^2 / 8N \right\}^{1/2} \quad (3)$$

where d_i is the difference between each duplicate value and N is the number of distinct experiments performed.

Table 3
Effect values and their standard errors for the interactions of the red dye with the chitosan beads

Effects	N_f (mg g^{-1})	$\Delta_{ads}G$ (kJ mol^{-1})
Average	28.00 ± 0.60	−45.48 ± 0.68
Principal		
C	52.72 ± 1.21	−8.00 ± 1.37
S	−27.39 ± 1.21	5.67 ± 1.37
T	−7.95 ± 1.21	−2.52 ± 1.37
Interactions		
C-S	−25.85 ± 1.21	4.63 ± 1.37
C-T	−7.03 ± 1.21	0.19 ± 1.37
S-T	2.97 ± 1.21	−1.43 ± 1.37
C-S-T	2.80 ± 1.21	−1.52 ± 1.37

The results obtained in a factorial design depend, in part, on the ranges of the factors studied. The chosen levels should be large enough to provoke response changes that are larger than experimental error. However, these differences should not be so large that quadratic or higher order effects due to the individual factors become important and invalidate the factorial model. Under these conditions factorial designs are particularly efficient for evaluating the principal effects of each factor and their interactions on adsorptions at the solid/solution interfaces, as well as those for academic and industrial processes [25].

The factorial design results are in Table 2 and the respective principal and interaction effects for the first factorial design study are presented in Table 3. The predicted adsorption values (N_f(p)) are also presented in Table 2. The effects error was 1.21 mg g^{-1}. If the interaction terms are left out of the model the error increases significantly to 7.88 mg g^{-1}.

On average, an increase in the red dye concentration causes an increase in the degree of adsorption observed. This is indicated by the principal effect for dye concentration of 52.72 mg g^{-1}. A similar behavior of the "dye concentration effect" has been detected in many adsorption studies [7,9,18–20]. When the initial concentration of dye increases, an increase in adsorption degree is found due to progressive occupation of the adsorption sites until the complete saturation of the adsorbent. So, the dynamic equilibria were influenced by the initial concentration [20]. Indeed, the quantitative adsorption, in one-variable-a-time methodology, is significantly changed when the initial dye concentrations are very different one another [26,27].

Surfactants are used for transportation or for the immobilization of the toxic chemicals such as heavy metal ions and dyes [7]. They can modify the surface properties of various materials, such as their surface charge or hydrophobicity/hydrophilicity. In this way, the sorption of various substances (typically organic compounds) can be supported (coadsorption), or even the sorption of normally non-retained species may be enabled (adsolubilization) [24–28]. However, a prediction of surfactant effects upon sorption is not straightforward, as several simultaneous and competitive mechanisms may be operating during the sorption process. In general, below the critical aggregation concentration (cac) of the dye/surfactant aggregates, the dye sorption increased with increasing surfactant concentration. Above the cac, on the other hand, the dye sorption was suppressed steeply as a result of complete micelle formation and dye solubilization [24–28]. The interactions of the dyes with the chitosan beads

occur by "free dyes" in solution and by the dye/DBS aggregates [28].

The cac of the dye/DBS aggregates were calculated using the surface tension technique and they were presented and discussed earlier [20,29]. Briefly, it is observed that the cac values of the red dye decrease from 124.52 to 88.50 mg L^{-1} with temperature increase, from 25 to 55 °C. This behavior has been related to the relatively ramified chemical structure of the red dye, which do not enable the formation of a great number of the dye/DBS hydrophobic interactions compared to other linear and/or planar molecules. So, the dye/surfactant hydrophobic interactions do not occur at higher extensions at high temperatures [26,27].

In this study, the red dye adsorption decreased in the presence of the anionic surfactant DBS. This is indicated by the principal effect for presence of DBS of −27.39 mg g^{-1}. The adsorption capacity of chitosan beads decreased in the presence of DBS as a result of the competitive adsorption for the same sites between the same charged dye and surfactant molecules. Additionally, the relatively large dye/DBS aggregates difficult the diffusion of large amounts of dye into the internal adsorption sites of the chitosan beads.

The adsorption decreased for the higher temperature value in the factorial design. The principal "temperature effect" in this factorial design is also an important factor for the removal of anionic dyes, but in a less extension than the factors "concentration" and "presence of surfactant". Most dyes adsorption works using chitosan as adsorbent have been shown an opposite situation showed in this work [27]. In fact, the increase in the uptake of dyes with temperature has been attributed to the enhanced diffusion of sorbate into the internal adsorption sites of chitosan [30]. So, the presence of the DBS aggregates seems to be also affected the role of temperature on the adsorption of red dye.

The interaction effect absolute values are much smaller than the initial dye concentration, the presence of DBS and temperature main effects. However, at the 95% confidence level, the interaction effect between initial dye concentration and surfactant is statistically important. The effect will be seen to be important for obtaining a quantitative model for this chitosan adsorption process.

A quantitative reduced model for the amounts of absorbed red dye can be written in terms of the statistically significant effects on N_f in Table 2 [23,24],

$$N_f = 28.20 + 26.36x_1 - 13.69x_2 - 12.93x_1x_2 - 3.98x_3 - 3.52x_1x_3 \quad (4)$$

where x_1, x_2 and x_3 are codified (±1) values of dye concentration, presence of surfactant and temperature, respectively.

Additional cubic polynomial models were also built, where values of N_f were calculated in relation to several initial red dye concentrations in solution (25–600 mg L^{-1}), in the absence and in the presence of DBS, at 25 and 55 °C, as following:

In the absence of DBS, 25 °C:

$$N_f = 3.45 - 0.02\ [\text{dye}] + 7.26 \times 10^{-4}\ [\text{dye}]^2 - 7.56 \times 10^{-7}\ [\text{dye}]^3, \quad R^2 = 0.9999 \quad (5)$$

In the absence of DBS, 55 °C:

$$N_f = 0.92 - 0.03\ [\text{dye}] + 2.24 \times 10^{-4}\ [\text{dye}]^2 - 1.45 \times 10^{-7}\ [\text{dye}]^3, \quad R^2 = 0.9998 \quad (6)$$

In the presence of DBS, 25 °C:

$$N_f = 2.37 - 0.01\ [\text{dye}] + 4.05 \times 10^{-4}\ [\text{dye}]^2 - 5.09 \times 10^{-7}\ [\text{dye}]^3, \quad R^2 = 0.9898 \quad (7)$$

In the presence of DBS, 55 °C:

$$N_f = 0.89 - 0.006\ [\text{dye}] + 2.40 \times 10^{-4}\ [\text{dye}]^2 - 3.13 \times 10^{-7}\ [\text{dye}]^3, \quad R^2 = 0.9907 \quad (8)$$

Taking into account that it is the first attempt to study adsorption of an anionic dye on chitosan beads simultaneously using all these factors, further statistical studies will point out more accurate modelings to evaluate the relative importance of each experimental factor of the quantitative anionic dyes adsorptions showed in this work. However, other adsorption parameters, using the factorial design results, can also be calculated and evaluated, as described hereafter.

3.3. Determination and analysis of thermodynamic energies for the red dye adsorption according to the factorial design

The thermodynamic parameters, namely the equilibrium constants (K), the enthalpy of adsorption ($\Delta_{ads}H$), the Gibbs free energies of adsorption ($\Delta_{ads}G$) and the entropy of adsorption ($\Delta_{ads}S$) were calculated as shown in Eqs. (9)–(12), using the average adsorption quantities of the factorial design matrix, in relation to the following general equilibrium [28–30]:

$$\text{Chitosan} - \text{NH}_{2(s)} + \text{dye (eq)}_{(aq)} \rightleftharpoons \text{Chitosan} - \text{NH}_2/\text{dye}_{(s)}$$

$$K = \frac{\theta}{(1-\theta)C_{eq}} \quad (9)$$

$$\ln\frac{K_{55}}{K_{25}} = \Delta_{ads}H\frac{(T_{55}-T_{25})}{R(T_{55}T_{25})} \quad (10)$$

$$\Delta_{ads}G = -RT\ \ln\ K \quad (11)$$

$$\Delta_{ads}G = \Delta_{ads}H - T\Delta_{ads}S \quad (12)$$

where θ is the fraction of adsorption that are occupied by red dye in relation to the available free NH_2 groups on chitosan after cross-linking reaction, or 3.10 mmol NH_2/chitosan mass. Thus, $\theta = N_f/(3.10\ \text{mmol NH}_2/\text{chitosan mass})$. C_{eq} is the equilibrium concentration (mol L^{-1}) of dye in solution, T is the solution temperature (Kelvin), which was used in relation to each factorial design and R is the universal gas constant (8.314 J K^{-1} mol^{-1}).

In univariate adsorption studies, the thermodynamic aspects of adsorption are directly related to the changes of the adsorption temperature [31]. However, from the results of the multivariate study found in this work, the effects of the concentration and the presence of surfactant were also very expressive in relation to the calculated error. So, the different values for the thermodynamic parameters of the red dye adsorption on chitosan beads can be due to the role of all principal and the interactive factors of the factorial design and not to the "temperature effect" alone [32].

Table 4 shows the calculated values of the thermodynamic parameters for the red dye adsorptions on the cross-linked chitosan beads. The equilibrium constants are found to be different from one another, due to the differences in the N_f values found in the factorial design results. The different tendencies of the solvent detachment from both the dye molecule and the interaction sites of the chitosan at 25 or 55 °C, as well as the different modes of interaction of the dye in relation to the adsorbent coverage have been also considered as important factors to produce different adsorption thermodynamic quantities [32,33].

The values of $\Delta_{ads}H$ indicate exothermic and endothermic adsorption processes for the factorial design experiments. One possible explanation of the exothermicity or endothermicity of heats of adsorption [34,35] is the well-known fact that dyes and carbohydrate materials are both well solvated in water. In order for the dyes to be adsorbed, they have to lose part of their hydration shell.

Table 4
Thermodynamic parameters of the adsorption of red dye in relation to the 2^3 factorial design results

Experiment	Var C	Var S	Var T	$\ln K$	$\Delta_{ads}H$[a] (kJ mol^{-1})	$-\Delta_{ads}G$ (kJ mol^{-1})	$\Delta_{ads}S$ (J K^{-1} mol^{-1})
1	−1	−1	−1	16.28	−2.70	40.32	135.3
2	1	−1	−1	21.94	−17.59	54.35	182.3
3	−1	1	−1	15.99	−4.25	39.63	133.0
4	1	1	−1	16.87	0.90	41.80	140.3
5	−1	−1	1	15.95	−2.70	43.50	132.6
6	1	−1	1	19.82	−17.59	54.50	164.8
7	−1	1	1	15.48	−4.25	42.22	128.7
8	1	1	1	16.98	0.90	46.30	141.2

[a] Taking into account the range of values for $\ln K$, $\Delta_{ads}G$ and $\Delta_{ads}S$, the $\Delta_{ads}H$ for the experiments 1–4 are considered similar for the experiments 5–8 with errors of ±5%.

The dehydration processes of the dyes and the adsorbent surface require energy. So, in some cases, the dehydration processes supersede the exothermicity of the adsorption processes. In summary, we may say that the removal of water from the dyes and the chitosan structure is essentially an endothermic process and it appears that endothermicity of the desolvation processes, in some cases in this study, exceeds that of the exothermicity provided by the heat of adsorption. However, we are unable to point out the extension of these desolvation processes, using the adsorption data of this work. We think that additional computational studies should be useful in the future, in order to estimate the endothermicity of the desolvation processes. The main difficulties are related to understanding the correct fraction of solvent released from both the dye molecules in solution and chitosan at a given temperature. The unreacted hydroxyl groups present on chitosan would also contribute to adsorption and release of water present on the chitosan [1,6]. The involved adsorption steps, at equilibrium conditions, can be stated, in a simplified manner, as follows [32,33]:

$$\text{Adsorbent} + \text{solvent} = \text{Adsorbent(solvent)} \quad (13)$$

$$\text{Adsorbent(solvent)} + \text{dye(solvent)} = \text{Adsorbent} - \text{dye} \\ \text{(solvent)} + \text{solvent} \quad (14)$$

As can be seen from Table 4, the positive $\Delta_{ads}S$ values indicate that entropy is also a driving force for adsorption [36].

For the sake of comparison, Table 5 presents comparative values of $\Delta_{ads}H$ for some dye-adsorbent interactions. In general, it has been observed that exothermic $\Delta_{ads}H$ values are found for dye adsorptions that occur, mainly, on the surfaces of low-size porous adsorbents. On the other hand, the diffusion of the dye molecules (or ions) into the internal parts of the adsorbent materials provokes endothermic and/or very small exothermic values of $\Delta_{ads}H$ [30–36]. So, the wide range of the comparative results of the $\Delta_{ads}H$ in Table 5 (some of them obtained by direct isothermal titration calorimetry) should be seen as evidence that the adsorption thermodynamic values are average results of both diffusional (endothermic) and chemical bonding (exothermic) processes [35]. In addition, the interactive role of the experimental variables, provided in the present work by the factorial design methodology, should also be taking into account to evaluate the changes of the $\Delta_{ads}H$ values.

The positive $\Delta_{ads}S$ values, as well as the relatively high magnitude of the negative $\Delta_{ads}G$ values found in this work have also been considered as the consequence of the presence of the red dye molecules, mainly, on the surface of the cross-linked chitosan beads [20,27,30,34]. Indeed, high negative $\Delta_{ads}G$ values (less than -25 kJ mol^{-1}) are found when adsorption occurs, mainly, on the surfaces of the adsorbents [16,36,37].

The thermodynamic results presented in present work are in good agreement with the adsorption studies found in literature [11,16,38]. However, only the factorial design methodology can determine the most important principal and interactive factors to change the adsorption thermodynamics at the solid/solution interface.

Table 5
Comparative values of $\Delta_{ads}H$ (kJ mol^{-1}) for some adsorbent/dye interactions from aqueous solutions

Adsorbent/adsorbate	$\Delta_{int}H$	Reference
Zeolite MCM-22/basic dye	+5.4	[39]
Carbon slurry/ethyl orange	−6.20	[38]
Carbon slurry/chrysoidine B	−0.70	[38]
Fly ash/basic fuchsin	21.4	[38]
Fly ash/methylene blue	76.1	[38]
Red mud/methylene blue	10.8	[38]
Coir pith/Congo red	7.71	[38]
Red mud/methylene blue	−31.0	[38]
Fullers earth/methylene blue	158	[38]
Bentonite/Nylosan red EBL	26.8	[40]
Bentonite/Nylosan blue EBL	12.2	[40]
Wool fibers/acid violet 17	20.9	[41]
Wool fibers/acid blue 90	23.3	[41]
Wool fibers/acid red 1	84.8	[41]
Wool fibers/direct red 80	49.5	[41]
74% Deacetylated chitosan/azonaphthalene-trisulfonate	−2.17	[42]
85% Deacetylated chitosan/azonaphthalene-trisulfonate	−23.4	[42]
Raw chitin powder/indigo carmine	−40.1	[40]
Raw chitosan powder/indigo carmine	−23.4	[27]
Raw chitosan powder/indigo carmine	−29.2	[43]
Chitosan beads/(low red dye concentration without DBS)	−2.70	This work
Chitosan beads/(high red dye concentration without DBS)	−17.6	This work
Chitosan beads/(low red dye concentration with DBS)	−4.25	This work
Chitosan beads/(high red dye concentration with DBS)	0.90	This work

In this work, the adsorption thermodynamics modeling was performed using the $\Delta_{ads}G$ values, since their values were obtained directly from the equilibrium constants (K). A quantitative reduced model for the $\Delta_{ads}G$ values is presented in Eq. (15), in terms of their statistically significant effects showed in Table 3 [23,24],

$$\Delta_{ads}G = -45.48 - 4.00x_1 + 2.84x_2 + 2.31x_1x_2 \quad (15)$$

It is noted that the adsorption of red dye, in relation to the $\Delta_{ads}G$ values point of view, is a complex phenomenon. The concentration of the dye and temperature work to increase the $\Delta_{ads}G$ in a negative sense. The principal effect of the presence of DBS increases the $\Delta_{ads}G$ values in the positive sense. Additionally, the interactive effect of the variables "concentration" and "presence of surfactant" also works to increase the $\Delta_{ads}G$ in the positive sense.

4. Conclusions

The results obtained in this study show that the changes proposed in the factorial design study affected the adsorption levels of the red dye by using cross-linked chitosan beads.

The results indicated that increasing the initial dye concentration from 25 to 600 mg L^{-1} decreases the dye adsorption/mass

ratio ($\mathrm{mol\,g^{-1}}$) whereas the presence of the surfactant DBS and a temperature increase of 25–35 °C increases it. The adsorption capacity of chitosan beads decreased in the presence of DBS as a result of the competitive adsorption for the same sites between the dye and surfactant molecules. The factorial experiments demonstrate the existence of a significant antagonistic interaction effect between the "concentration" and "surfactant" factors. The quantitative adsorption (N_f) modeling present good correlations with the experimental data.

It is noted that the values of $\Delta_{ads}H$ indicate exothermic and endothermic adsorption processes for the factorial design experiments. The adsorption thermodynamic values are average results of both diffusional (endothermic) and chemical bonding (exothermic) processes. The concentration of the dye and temperature work to increase the $\Delta_{ads}G$ in a negative sense. The principal effect of the presence of DBS increases the $\Delta_{ads}G$ values in the positive sense. The negative values of $\Delta_{ads}G$ indicate that the adsorption processes are thermodynamically spontaneous. The positive $\Delta_{ads}S$ values indicate that entropy is also a driving force for adsorption.

Acknowledgements

The authors thank the Brazilian National Agency CNPq for fellowships and financial support to A.R.C. and E.F.S.V.

References

[1] E. Guibal, Interactions of metal ions with chitosan-based sorbents: a review, Separ. Purif. Technol. 38 (2004) 43–74.
[2] G. Crini, Recent developments in polysaccharide-based materials used as adsorbents in wastewater treatment, Prog. Polym. Sci. 30 (2005) 38–70.
[3] A.J. Varma, S.V. Deshpande, J.F. Kennedy, Metal complexation by chitosan and its derivatives: a review, Carbohydr. Polym. 55 (2004) 77–93.
[4] V.L. Gonçalves, M.C.M. Laranjeira, V.T. Fávere, Effect of crosslinking agents on chitosan microspheres in controlled release of diclofenac sodium, Polímers: Sci. Technol 15 (2005) 6–12 (in Portuguese).
[5] R.A.A. Muzzarelli, Natural Chelating Polymers: Alginic Acid, Chitin and Chitosan, Oxford University Pergamon Press, England, 1973.
[6] E. Guibal, Heterogeneous catalysis on chitosan-based materials: a review, Prog. Polym. Sci. 30 (2005) 71–109.
[7] H.K. No, S.P. Meyers, Application of chitosan for treatment of wastewaters, Rev. Environ. Contam. Toxicol. 163 (2000) 1–28.
[8] W.Q. Sun, G.F. Payne, M.S.G.L. Moas, J.H. Chu, K.K. Wallace, Tyrosinase reaction/chitosan adsorption for removing phenols from wastewater, Biotechnol. Prog. 8 (1992) 179–186.
[9] R.S. Juang, F.C. Wu, R.L. Tseng, Solute adsorption and enzyme immobilization on chitosan beads prepared from shrimp shell wastes, Biores. Technol. 80 (2001) 187–193.
[10] J.M.C.S. Magalhães, A.A.S.C. Machado, Urea potentiometric biosensor based on urease immobilized on chitosan membranes, Talanta 47 (1998) 183–191.
[11] I.S. Lima, C. Airoldi, A thermodynamic investigation on chitosan–divalent cation interactions, Thermochim. Acta 421 (2004) 133–139.
[12] N. Karatepe, Adsorption of a non-ionic dispersant on lignite particle surfaces, Energy Conv. Manag. 44 (2003) 1275–1284.
[13] S. Chegrouche, A. Bensmaili, Removal of Ga(III) from aqueous solution by adsorption on activated bentonite using a factorial design, Water Res. 36 (2002) 2898–2904.
[14] G. Annadurai, R.S. Juang, D.J. Lee, Factorial design analysis for adsorption of dye on activated carbon beads incorporated with calcium alginate, Adv. Environ. Res. 6 (2002) 191–198.
[15] G. Nicholls, B.J. Clark, J.E. Brown, Solid-phase extraction and optimized separation of doxorubicin, epirubicin and their metabolites using reversed-phase high-performance liquid chromatography, J. Pharm. Biom. Anal. 10 (1992) 949–957.
[16] O.A.C. Monteiro Jr., C. Airoldi, Some thermodynamic data on copper–chitin and copper–chitosan biopolymer interactions, J. Colloid Interface Sci. 212 (1999) 212–219.
[17] O. Leal, C. Bolévar, C. Ovalles, J.J. Garcia, Y. Espidel, Reversible adsorption of carbon dioxide on amine surface-bonded silica gel, Inorg. Chim. Acta 240 (1995) 183–189.
[18] E.C.N. Lopes, F.S.C. dos Anjos, E.F.S. Vieira, A.R. Cestari, An alternative Avrami equation to evaluate kinetic parameters of the interaction of Hg(II) with thin chitosan membranes, J. Colloid Interface Sci. 263 (2003) 542–547.
[19] A.R. Cestari, E.F.S. Vieira, E.S. Silva, Interactions of anionic dyes with silica-aminopropyl 1. A quantitative multivariate analysis of equilibrium adsorption and adsorption Gibbs free energies, J. Colloid Interface Sci. 297 (2006) 22–30.
[20] A.R. Cestari, E.F.S. Vieira, A.A. Pinto, E.C.N. Lopes, Multistep adsorption of anionic dyes on silica/chitosan hybrid: 1. Comparative kinetic data from liquid- and solid-phase models, J. Colloid Interface Sci. 292 (2005) 363–372.
[21] Yong-Xiao Bai, Yan-Feng Li, Preparation and characterization of crosslinked porous cellulose beads, Carbohydr. Polym. 64 (2006) 402–407.
[22] K. Ravikumar, S. Krishnan, S. Ramalingam, K. Balu, Optimization of process variables by the application of response surface methodology for dye removal using a novel adsorbent, Dyes Pigm. 72 (2007) 66–74.
[23] G.P.G. Box, J.S. Hunter, W.G. Hunter, Statistics for Experimenters: Design, Innovation and Discovery, 2nd ed., John Wiley & Sons, USA, 2005.
[24] R.E. Bruns, I.S. Scarminio, B. de Barros Neto, Statistical Design—Chemometrics, Elsevier, Amsterdam, 2006.
[25] A.R. Cestari, E.F.S. Vieira, A.J.P. Nascimento, C. Airoldi, New factorial designs to evaluate chemisorption of divalent metals on aminated silicas, J. Colloid Interface Sci. 241 (2001) 45–51.
[26] J. Shen, Z. Duvnjak, Adsorption kinetics of cupric and cadmium ions on corncob particles, Proc. Biochem. 40 (2005) 3446–3454.
[27] F.S.C. dos Anjos, E.F.S. Vieira, A.R. Cestari, Interaction of indigo carmine dye with chitosan evaluated by adsorption and thermochemical data, J. Colloid Interface Sci. 253 (2002) 243–246.
[28] S.S. Tahir, N. Rauf, Thermodynamic studies of Ni(II) adsorption onto bentonite from aqueous solution, J. Chem. Thermodyn. 35 (2003) 2003–2009.
[29] E. Gimenez-Martin, M. Espinosa-Jiménez, Influence of tannic acid in leacril/rhodamine B system: thermodynamics aspects, Colloids Surfaces A 270/271 (2005) 93–101.
[30] R. Goobes, G. Goobes, C.T. Campbell, P.S. Stayton, Thermodynamics of statherin adsorption onto hydroxyapatite, Biochemistry 45 (2006) 5576–5586.
[31] Y.-S. Ho, A.E. Ofamaja, Kinetics and thermodynamics of lead ion sorption on palm kernel fibres from aqueous solution, Proc. Biochem. 40 (2005) 3455–3461.
[32] J. Romero-González, J.R. Peralta-Videa, E. Rodríguez, S.L. Ramirez, J.L. Gardea-Torresdey, Determination of thermodynamic parameters of Cr(VI) adsorption from aqueous solution onto *Agave lechuguilla* biomass, J. Chem. Thermodyn. 37 (2005) 343–347.
[33] A.R. Cestari, C. Airoldi, R.E. Bruns, A fractional factorial design applied to organofunctionalized silicas for adsorption optimization, Colloids Surfaces A 117 (1996) 7–13.
[34] A.R. Cestari, E.F.S. Vieira, C.R.S. Mattos, Thermodynamics of the Cu(II) adsorption on thin vanillin-modified chitosan membranes, J. Chem. Thermodyn. 38 (2006) 1092–1099.
[35] A.R. Cestari, E.F.S. Vieira, A.G.P. dos Santos, J.A. Mota, V.P. de Almeida, Adsorption of anionic dyes on chitosan beads. 1. The influence of the chemical structures of dyes and temperature on the adsorption kinetics, J. Colloid Interface Sci. 280 (2004) 380–386.
[36] J. Wu, Yu. Han-Qing, Biosorption of 2,4-dichlorophenol from aqueous solution by *Phanerochaete chrysosporium* biomass: isotherms, kinetics and thermodynamics, J. Hazard. Mater. B 137 (2006) 498–508.
[37] E.F.S. Vieira, A.R. Cestari, J.A. Simoni, C. Airoldi, Thermochemical data for interaction of some primary amines with complexed mercury on mercapto-modified silica gel, Thermochim. Acta 399 (2003) 121–126.
[38] A. Ramesh, D.J. Lee, J.W.C. Wong, Thermodynamic parameters for adsorption equilibrium of heavy metals and dyes from wastewater with low-cost adsorbents, J. Colloid Interface Sci. 291 (2005) 588–592.
[39] S. Wang, H. Li, L. Xu, Application of zeolite MCM-22 for basic dye removal from wastewater, J. Colloid Interface Sci. 295 (2006) 71–78.
[40] A.S. Özcan, A. Özcan, Adsorption of acid dyes from aqueous solutions onto acid-activated bentonite, J. Colloid Interface Sci. 276 (2004) 39–46.
[41] M. Saleem, T. Pirzada, R. Qadeer, Sorption of some azo-dyes on wool fiber from aqueous solutions, Colloids Surfaces A 260 (2005) 183–188.
[42] T.K. Saha, S. Karmaker, H. Ichikawa, Y. Fukumori, Mechanisms and kinetics of trisodium 2-hydroxy-1,1′-azonaphthalene-3,4′,6-trisulfonate adsorption onto chitosan, J. Colloid Interface Sci. 286 (2005) 433–439.
[43] A.G.S. Prado, J.D. Torres, E.A. Faria, S.C.L. Dias, Comparative adsorption studies of indigo carmine dye on chitin and chitosan, J. Colloid Interface Sci. 277 (2004) 43–47.